

# 基于碳氮双键构建粘度响应探针：“高保真”监测急性肝损伤研究

王 盛, 颜健奇, 倪朝舜, 甘亚兵\*, 聂立波\*

湖南工业大学生物与医学工程学院, 湖南 株洲

收稿日期: 2026年3月8日; 录用日期: 2026年4月30日; 发布日期: 2026年5月12日

## 摘 要

近年来, 药物滥用、病毒感染及过度饮酒等致病因素的叠加, 导致急性肝损伤的发病率持续攀升。当前临床诊断主要依赖血清生化指标检测和影像学评估, 但这些手段在早期阶段常因灵敏度不足、特异性有限而导致漏诊, 致使患者错过最佳干预时机。发展兼具时效性与精准度的早期诊断技术, 已成为临床肝病诊疗领域亟待突破的核心问题。本研究成功开发了一种基于碳氮双键(C=N)旋转机制的新型近红外(NIR)荧光探针, 用于超灵敏响应微环境粘度变化。该探针展现出优异的选择性、超高灵敏度、出色的光稳定性及宽pH耐受性等特性。结果表明, 它能有效监测由脂多糖(LPS)诱导的炎症模型中细胞粘度的升高, 并成功应用于对乙酰氨基酚(APAP)诱导的肝损伤模型中细胞内粘度的实时成像监测。该探针为研究细胞粘度相关的生理病理过程, 特别是为急性肝损伤的早期监测提供了有力手段。

## 关键词

急性肝损伤, 荧光探针, 近红外, 粘度, 可视化监测

# Construction of Viscosity-Responsive Probes Based on Carbon-Nitrogen Double Bonds: A Study on “High-Fidelity” Monitoring of Acute Liver Injury

Sheng Wang, Jianqi Yan, Chaoshun Ni, Yabing Gan\*, Libo Nie\*

School of Biological Science and Medical Engineering, Hunan University of Technology, Zhuzhou Hunan

Received: March 8, 2026; accepted: April 30, 2026; published: May 12, 2026

\*通讯作者。

文章引用: 王盛, 颜健奇, 倪朝舜, 甘亚兵, 聂立波. 基于碳氮双键构建粘度响应探针: “高保真”监测急性肝损伤研究[J]. 生物医学, 2026, 16(3): 359-368. DOI: 10.12677/hjbm.2026.163038

## Abstract

In recent years, the incidence rate of acute liver injury has been continuously rising due to the combination of pathogenic factors such as drug abuse, viral infection, and excessive alcohol consumption. Current clinical diagnosis mainly relies on serum biochemical indicator testing and imaging assessments, but these methods often lead to missed diagnoses in the early stages due to insufficient sensitivity and limited specificity, resulting in patients missing the optimal intervention window. Developing early diagnostic techniques that are both timely and precise has become a core issue urgently requiring breakthroughs in the field of clinical liver disease diagnosis and treatment. This study successfully developed a novel near-infrared (NIR) fluorescent probe based on the rotation mechanism of carbon-nitrogen double bonds (C=N) for ultra-sensitive response to changes in microenvironment viscosity. The probe exhibits excellent selectivity, ultra-high sensitivity, outstanding photostability, and wide pH tolerance. The results demonstrate that it can effectively monitor the increase in cell viscosity in an inflammation model induced by lipopolysaccharide (LPS) and has been successfully applied to real-time imaging monitoring of intracellular viscosity in a liver injury model induced by acetaminophen (APAP). This probe provides a powerful tool for studying physiological and pathological processes related to cell viscosity, especially for the early monitoring of acute liver injury.

## Keywords

Acute Liver Injury, Fluorescent Probe, Near-Infrared, Viscosity, Visual Monitoring

Copyright © 2026 by author(s) and Hans Publishers Inc.

This work is licensed under the Creative Commons Attribution International License (CC BY 4.0).

<http://creativecommons.org/licenses/by/4.0/>



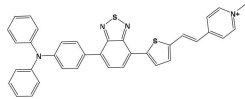
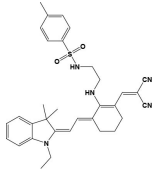
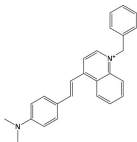
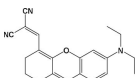
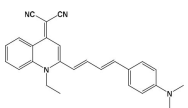
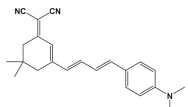
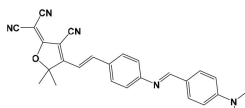
Open Access

## 1. 引言

肝脏是维持代谢稳态和解毒的核心器官，在异生物质清除、生物合成和代谢调节中发挥着至关重要的作用[1] [2]。然而，在持续的伤害(如病毒感染、药物毒性和酒精滥用)下，全球肝病发病率持续上升，构成了重大的公共卫生负担[3]。譬如急性肝损伤(ALI)，目前已成为临床常见的肝病之一，受到全世界范围的广泛关注[4]-[8]，其导致肝细胞坏死、肝功能衰竭，并可能引发多器官功能障碍综合征。因此，急性肝损伤的早期诊断与干预至关重要[9]。细胞内粘度作为关键微环境参数，对于多种依赖扩散的生物学过程，包括电子传递、代谢废物运输以及细胞内乃至细胞间信号传导都十分重要[10]-[15]，其异常升高与急性肝损伤密切相关：肝细胞代谢紊乱引发氧化应激和炎症因子累积，破坏内稳态并导致粘度显著增加[16] [17]。精准监测粘度变化对急性肝损伤早期识别与疗效评估具有重要价值[18] [19]。

传统粘度检测技术(如流变学)操作复杂、灵敏度低，且难以实现细胞/组织水平的实时可视化监测。因此，急性肝损伤的早期诊断的可靠性和快速性仍然具有挑战性[20]-[23]。近红外荧光探针因其高灵敏度、操作简便、实时监测、良好的组织穿透性及低背景干扰等优势成为理想工具[24]-[28]，例如下表 1 所示。虽有研究尝试将其用于急性肝损伤粘度检测，但现有探针仍然存在一些局限：首先，其中一些荧光探针灵敏度不足，难以检测生理或病理范围内的细微粘度变化。其次，一些探针选择性欠佳，易受其他生物活性分子干扰。第三，应用局限，缺乏面向急性肝损伤模型及药物干预条件下的粘度动态成像研究[21] [29]-[31]。因此，开发一种高灵敏度的粘度探针用于急性肝损伤成像的情势十分紧迫，具有重要意义。

**Table 1.** Near-infrared probes for viscosity  
**表 1.** 粘度的近红外探针

Probe structure	$\lambda_{em}$	Detection range	Biological applications	Ref.
	680 nm	1.2 cP to 430 cP	Cell/Mice	[32]
	626 nm	3 cP to 647 cP	Cell/Mice	[33]
	676 nm	1.5 cP to 1099.5 cP	Cell/Zebrafish	[34]
	667 nm	1.29 cP to 937 cP	Cell/Mice	[35]
	650 nm	1.05 cP to 945 cP	Cell	[36]
	700 nm	1.05 cP to 695.4 cP	Cell/Mice	[37]
	650 nm	0.59 cP to 945 cP	Cell	This work

针对上述瓶颈,本研究设计了一种基于碳氮双键旋转的超灵敏近红外荧光探针,如图 1。该探针在高粘度环境中通过分子内运动受限机制,荧光强度显著增强[29] [38]。本研究旨在合成一种具有高灵敏度、高选择性、优异光稳定性、宽 pH 耐受性及较低生物毒性的荧光探针,对急性肝损伤细胞模型中粘度变化的精准、实时监测,为急性肝损伤的精准诊疗提供一种新的分子工具。

## 2. 实验仪器、材料与方

本实验所用化学试剂购自阿拉丁(中国上海),使用前无需进一步纯化。实验细胞购自中国典型培养物保藏中心(中国武汉),并用含有 10%胎牛血清(Grand Island, Gibco BRL, NY, 美国)、1%链霉素(100 U/mL)和 1%青霉素(100 ug/mL)的 DMEM 培养液培养并传代。实验用水采用超纯水(18.25 M $\Omega$ ·cm)。反应产物采用薄层色谱法进行监测,并用硅胶(200~300 目)进行柱层析纯化。荧光光谱采用日立 F-7100 分光光度计(Hitachi Ltd., 日本)进行分析,使用 10 mm 标准石英比色皿(PMT 电压, 650 V; 扫描速度: 1200 nm/min; 延时, 0 s; 响应, 2 s)。以四甲基硅烷(TMS)为内标,在 BRUKER AVANCE-500 光谱仪上获得  $^1\text{H}$  NMR 和  $^{13}\text{C}$  NMR 谱。采用荧光共聚焦显微镜系统(Leica SP8, 德国)进行细胞成像实验。

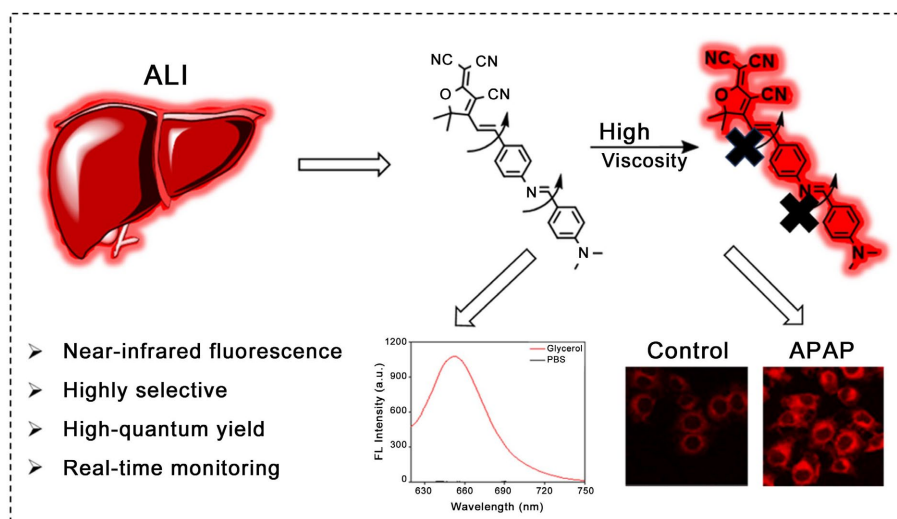


Figure 1. Design of the probe

图 1. 探针的设计

## 2.1. 探针的合成及表征

合成：将 900 mg 3-羟基-3-甲基-丁酮、1.2 g 丙二腈和 71.41 mg 乙醇钠混合加入 100 mL 的圆底烧瓶中，加入 10 mL 乙醇溶解，常温搅拌 0.5 h，升温到 50℃ 下反应过夜，过滤，旋干后与 122 mg 对 - 二甲氨基苯甲醛混合，加入 8 mL 乙醇溶解，在 95℃ 下恒温反应过夜，旋干，柱层析纯化后与 50 mg 的对 - 二甲氨基苯甲醛混合，再加入 10 mL 乙醇溶解并搅拌，在 60℃ 下搅拌恒温反应过夜，通过柱层析纯化，旋干得到探针 1 (如图 2)，进行核磁表征。

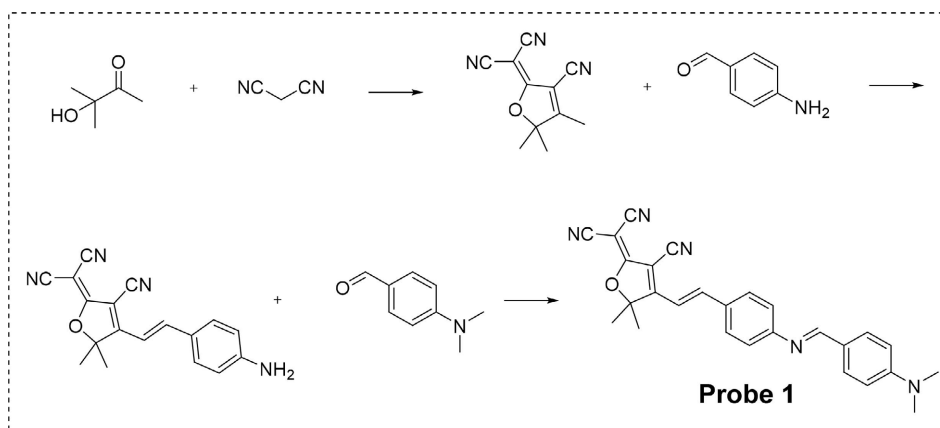


Figure 2. Synthesis route of fluorescent probe 1

图 2. 荧光探针 1 的合成路线

## 2.2. 探针的荧光性能实验

探针 1 的标准溶液(1 mM)采用二甲基亚砷(DMSO)配制。实验用到的活性氧、活性硫、氨基酸、金属盐离子等的标准溶液(10 mM)均用去离子水配制。这些标准溶液随后被稀释至所需的测量浓度。测试溶液的制备方法如下：将 20  $\mu$ L 探针 1 溶液(1  $\mu$ M)和适量的分析物溶液加入到一个试管中，然后使用不同的溶液将其稀释至 2 mL。在室温下、指定时间内，记录荧光光谱。

### 2.3. 细胞培养

HepG2 在 37℃ 和含 5% 的 CO<sub>2</sub> 的恒温培养箱中, 使用含有 10% 胎牛血清(Grand Island, Gibco BRL, NY, 美国)、1% 链霉素(100 U/mL)和 1% 青霉素(100 ug/mL)的 DMEM 培养液培养人肝癌细胞(HepG2), 隔 2~3 天进行传代。

### 2.4. 细胞毒性实验

细胞毒性通过 MTT (3-(4,5-二甲基-2-噻唑基)-2,5-二苯基四唑溴盐)测定法进行评估。HepG2 细胞在 96 孔板中培养, 直至达到 60%~70% 的细胞融合度, 然后用不同浓度的探针 1 (0~10 μM) 孵育 24 h。随后加入 200 μL MTT (0.5 mg/mL), 在 37℃ 下孵育 4 h, 用多通道微孔板读数仪(SpectraMax i3, 美国)在 590 nm 处测量吸光度。

### 2.5. 细胞荧光成像实验

探究不同温度对细胞质粘度的影响, 以及探针的检测效果: HepG2 细胞在不同温度(4℃、25℃、37℃) 下与 5 μM 探针孵育 30 min 后成像。

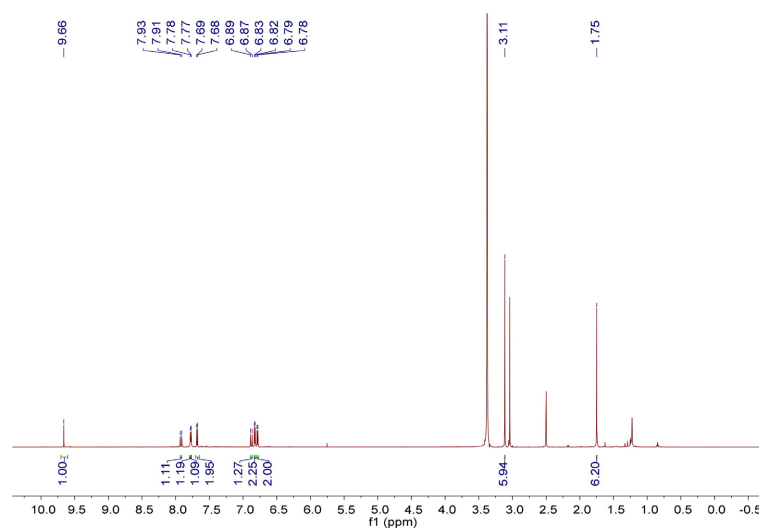
利用脂多糖(LPS)诱导细胞炎症, 探究炎症发生时细胞质的粘度变化: 对照组: 细胞与 5 μM 探针孵育 30 min; LPS 组: 用 LPS 预处理细胞 30 min, 然后用探针孵育 30 min。LPS + NAC (N-乙酰半胱氨酸, 缓解细胞内炎症反应)组: 用 LPS + NAC 预处理细胞 30 min, 用探针孵育 30 min, 随后进行荧光成像。

利用对乙酰氨基酚(APAP)建立肝损伤模型, 评估探针用于急性肝损伤模型的实时监测能力: 对照组: 用探针处理细胞 30 min; APAP 组: 细胞与不同浓度的 APAP (200/500/1000 μM) 共孵育 8 h, 然后用探针处理 30 min; NAC 组: 用 NAC (200 μM) 预处理 1 h 的细胞, 然后与 APAP (1000 μM) 共孵育 8 h, 随后进行荧光成像。

## 3. 结果与分析

### 3.1. 探针的核磁共振

为了确保探针的正确合成, 我们对探针进行了核磁表征, 得到的数据如图 3。可以看出探针的正确合成, 以及纯化后的探针纯度较高, 可以用于后续的分析实验。



(a)

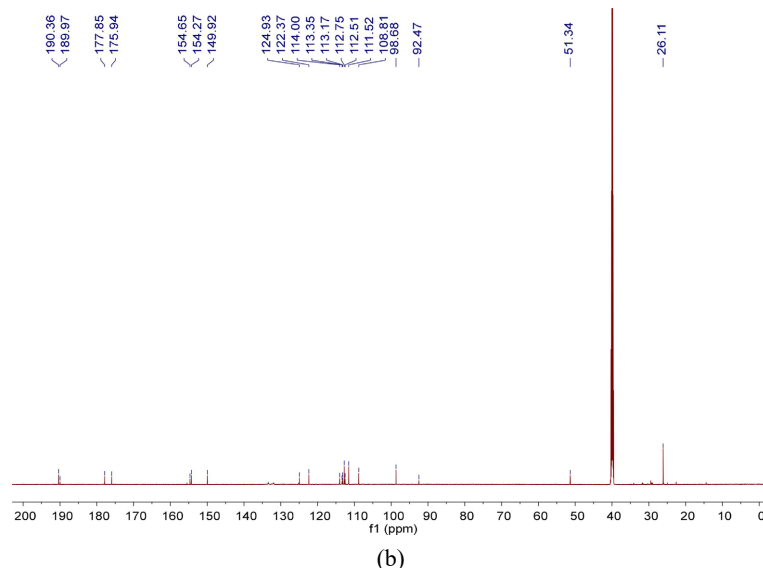
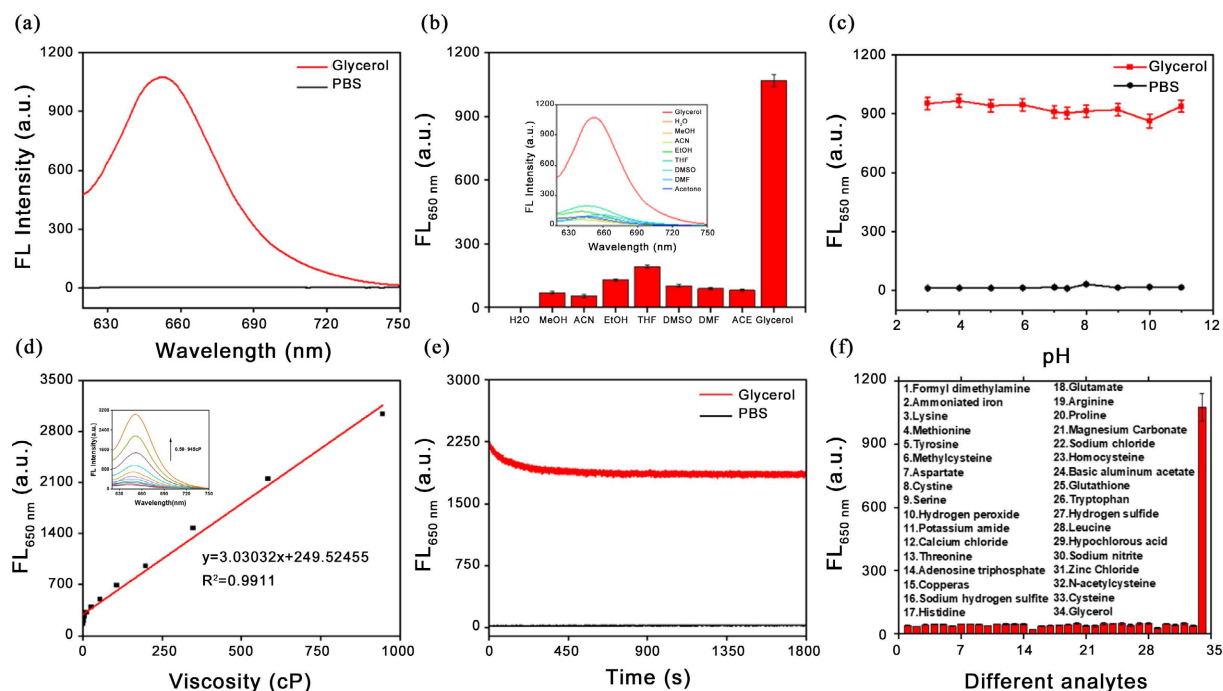


Figure 3. (a)  $^1\text{H}$  NMR spectrum of probe 1; (b)  $^{13}\text{C}$  NMR spectrum of probe 1

图 3. (a) 探针 1 的氢核磁谱; (b) 探针 1 的碳核磁谱

### 3.2. 探针的荧光性能

首先, 为验证该探针对接度的响应, 我们在室温下于甘油与 PBS (pH = 7.4, 10 mM, v:v = 5:5) 体系中研究其荧光特性。如图 4(a) 所示, 在激发波长 600 nm 下, 探针处于高粘度甘油中时在 652 nm 处出现明显的“荧光开启”效应; 而在 PBS 中几乎无荧光信号。与 PBS 相比, 甘油体系中荧光强度增强 625 倍, 表明该探针可实现高信噪比的粘度检测。接下来, 为了进一步验证探针在不同溶剂下的光学特性, 我们对探针在不同溶剂中的荧光进行了分析。如图 4(b) 所示, 当探针处于不同溶剂中时, 探针激发的荧光强度不同; 而只当探针处于甘油中时, 其激发的荧光强度显著增强, 表明该探针荧光强度与其处介质极性无关, 只对粘度具有较强的选择性, 能够有效响应粘度变化并实现检测。更进一步地, 我们对探针在不同 pH 条件下于 PBS 和甘油中的稳定性进行了分析。由图 4(c) 所示, 当探针处于 PBS 中, 在不同 pH 条件下探针激发的荧光强度相对稳定且较低; 当探针处于甘油中时, 在不同 pH 条件下探针激发的荧光强度均较高, 说明探针本身在不同 pH 条件下荧光强度较稳定, 能够有效检测粘度变化。为了精确评估探针荧光强度和粘度的线性关系, 通过逐步向甲醇 - 甘油体系中增加甘油比例来增加粘度, 并在不同粘度下记录了探针的荧光光谱。随着粘度从 0.59 cP 逐渐增到 945 cP, 该峰值逐渐增大, 进一步的线性回归分析如图 4(d) 显示, 荧光强度与粘度之间存在高度线性相关性。粘度体系在 0.59~945 cP 范围内遵循方程  $y = 249.52455x + 3.03032$  ( $R^2 = 0.9911$ ), 表明该荧光探针对接度展现了极好的灵敏度。接下来, 我们对探针进行了光稳定性考察, 如图 4(e) 所示, 在 650 nm 处, 当该探针处于 PBS 中时, 荧光强度在 0 至 1800 s 的时间范围内保持稳定且显示出较低的荧光强度; 当该探针处于甘油中时, 初始时刻荧光强度显著增强, 随后随着时间推移先逐渐减弱后趋于稳定。结果表明, 探针在粘度中, 随着时间的推移, 仍具有较高的荧光强度, 充分证实了该探针具备优异的光稳定性。最后, 为了评估探针在复杂环境中对接度变化的选择性响应能力, 我们研究了各种干扰物质对其荧光光谱的影响, 包括活性氧、活性硫、金属离子和氨基酸等多种物质, 如图 4(f) 所示, 当探针处于粘度较大的溶液中时可诱导明显的荧光开启反应, 而在与其他分析物接触则没有表现出明显的荧光变化, 这表明探针检测粘度时, 具有良好的选择性, 在存在干扰物质的情况下, 探针仍能够准确检测复杂系统中的粘度。



**Figure 4.** (a) Fluorescence spectra of the probe in glycerol and in PBS; (b) Fluorescence intensity of the probe in different solvents; (c) Effect of pH on the fluorescence intensity of the probe; (d) Linear relationship between  $\log(\text{fluorescence intensity})$  and  $\log(\text{viscosity})$ ; (e) Photostability experiment of the probe under continuous laser irradiation for 30 minutes at different viscosities; (f) Fluorescence intensity of the probe towards the analyte ( $\lambda_{\text{ex}} = 600 \text{ nm}$ )

**图 4.** (a) 探针在甘油和探针在 PBS 中的荧光光谱; (b) 探针在不同溶剂中的荧光强度; (c) pH 值对探针荧光强度的影响; (d)  $\log(\text{荧光强度})$ 与  $\log(\text{粘度})$ 的线性关系; (e) 探针在不同粘度下连续激光照射 30 min 的光稳定性实验; (f) 探针与分析物的荧光强度( $\lambda_{\text{ex}} = 600 \text{ nm}$ )

### 3.3. 细胞毒性

基于该探针对粘度检测具有优异的光学特性, 我们进一步通过共聚焦荧光成像评估其监测细胞内粘度变化的潜在应用。首先采用 MTT 法评估探针的细胞毒性。结果表明, 在  $\leq 10 \mu\text{M}$  条件下细胞存活率均高于 90%, 说明探针对活细胞无显著细胞毒性, 可用于后续生物实验(图 5)。后续实验中, 我们选择  $5 \mu\text{M}$  探针用于细胞成像。

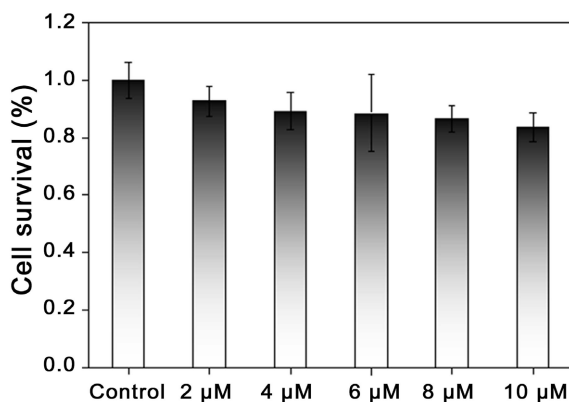


**Figure 5.** Cell survival rate under different concentrations (2, 4, 6, 8, 10  $\mu\text{M}$ ) of probe

**图 5.** 不同探针浓度(2, 4, 6, 8, 10  $\mu\text{M}$ )下的细胞存活率

### 3.4. 细胞荧光成像

为研究细胞质粘度的动态变化,将 HepG2 细胞在不同温度下与探针孵育 30 min 后成像。如图 6(a)所示,随着温度的降低,分子运动受限、细胞内环境粘度增加,荧光信号逐渐增强,说明探针可灵敏地响应细胞粘度变化。随后,我们用 LPS 诱导构建炎症模型,与对照组相比,LPS 刺激后细胞荧光信号增强;再加入 NAC 干预后,荧光强度减弱,说明炎症过程可引起细胞内粘度升高且 NAC 可部分逆转(图 6(b))。进一步地,为评估探针用于急性肝损伤模型的实时监测能力,我们建立了 APAP 诱导的 HepG2 细胞损伤模型。细胞用不同浓度的 APAP 处理后,再用探针检测荧光信号。结果显示(图 6(c)),荧光信号随 APAP 浓度升高而增强;在 NAC 预处理条件下,APAP 诱导的荧光增强被显著削弱,表明探针可直观检测细胞损伤模型中粘度的动态变化。综上,该探针可作为敏感分子工具用于细胞粘度成像,以区分不同程度的肝损伤,并为相关疾病的分子成像诊断提供有效手段。

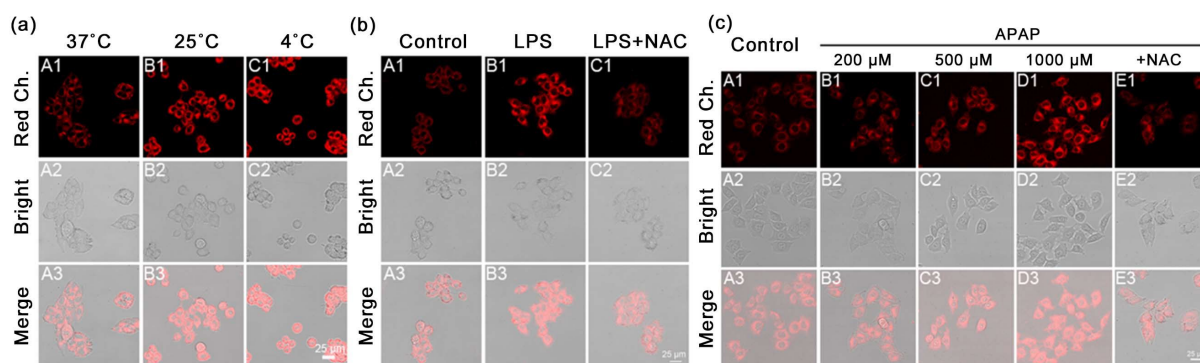


**Figure 6.** (a) Change in probe fluorescence intensity with temperature in cells at different temperatures; (b) Fluorescence imaging maps of viscosity in a cell inflammation model induced by lipopolysaccharide; (c) Fluorescence imaging maps of viscosity in a cell inflammation model induced by APAP

**图 6.** (a) 细胞在不同温度下,探针荧光强度随温度的变化;(b) 脂多糖诱导的细胞炎症模型中粘度的荧光成像图;(c) APAP 诱导的细胞炎症模型中粘度的荧光成像图

## 4. 总结

本研究开发了一种基于碳氮双键的超灵敏近红外粘度监测荧光探针,结果表明其具有优异的光学特性、良好的灵敏度和选择性,以及优异的光稳定性和 pH 耐受性,可实现对粘度的动态、准确检测。在肝损伤细胞模型中,该探针以良好的时间和空间分辨率监测了肝损伤过程中粘度的变化,表明粘度与肝损伤的严重程度密切相关。该探针为研究细胞粘度相关生理病理过程,特别是为急性肝损伤的早期监测提供了有力手段。

## 参考文献

- [1] Robinson, M.W., Harmon, C. and O'Farrelly, C. (2016) Liver Immunology and Its Role in Inflammation and Homeostasis. *Cellular & Molecular Immunology*, **13**, 267-276. <https://doi.org/10.1038/cmi.2016.3>
- [2] Sun, J., Cao, L., Dong, M., Liu, Y., Wang, Y. and Zhan, Y. (2026) HOCL and Viscosity Dual-Responsive Fluorescent Probe for Accurate Discrimination between Early Hepatocellular Carcinoma and Acute Liver Injury. *Materials Today Bio*, **37**, Article 102816. <https://doi.org/10.1016/j.mtbio.2026.102816>
- [3] Tak, J., Kim, Y.S. and Kim, S.G. (2025) Roles of X-Box Binding Protein 1 in Liver Pathogenesis. *Clinical and Molecular Hepatology*, **31**, 1-31. <https://doi.org/10.3350/cmh.2024.0441>
- [4] 尹一峰, 胡启辉, 杜毅超, 等. 细胞外基质在肝细胞性肝癌发生发展过程中的作用[J]. 中国普通外科杂志, 30(1): 91-97.

- [5] 刘双庆, 杨建中, 杨婷, 等. 成人急性肝损伤诊疗急诊专家共识[J]. 中国急救医学, 2024, 44(1): 5-12.
- [6] Paul, B.W. and Merrie, M. (2018) Mechanisms of Drug-Induced Liver Injury. In: Schiff, E.R., Maddrey, W.C. and Reddy, K.R., Eds., *Schiff's Diseases of the Liver, Twelfth Edition*, John Wiley & Sons Ltd., 774-798.
- [7] Xu, J.J., Diaz, D. and O'Brien, P.J. (2004) Applications of Cytotoxicity Assays and Pre-Lethal Mechanistic Assays for Assessment of Human Hepatotoxicity Potential. *Chemico-Biological Interactions*, **150**, 115-128. <https://doi.org/10.1016/j.cbi.2004.09.011>
- [8] Pugh, A.J., Barve, A.J., Falkner, K., Patel, M. and McClain, C.J. (2009) Drug-Induced Hepatotoxicity or Drug-Induced Liver Injury. *Clinics in Liver Disease*, **13**, 277-294. <https://doi.org/10.1016/j.cld.2009.02.008>
- [9] Qin, J., Kong, F., Huang, J., Xiao, B., Bian, Y. and Shao, C. (2025) Lysosome-Targeted Dual-Locked NIR Fluorescent Probe for Visualization of H<sub>2</sub>S and Viscosity in Drug-Induced Liver Injury and Tumor Models. *Analytica Chimica Acta*, **1337**, Article 343558. <https://doi.org/10.1016/j.aca.2024.343558>
- [10] Zhang, X., Wu, W., Wei, Y., Zhang, Y., Nie, X., Sun, X., *et al.* (2024) A FRET-Based Multifunctional Fluorescence Probe for the Simultaneous Detection of Sulfite and Viscosity in Living Cells. *Bioorganic Chemistry*, **148**, Article 107423. <https://doi.org/10.1016/j.bioorg.2024.107423>
- [11] Sun, X., Wang, J., Shang, Z., Wang, H., Wang, Y. and Shuang, S. (2024) A Triphenylamine-Thiophene-Based Fluorescent Probe for the Dual-Channel Detection and Imaging of Hypochlorite and Viscosity in Live Cells. *Journal of Molecular Liquids*, **402**, Article 124788. <https://doi.org/10.1016/j.molliq.2024.124788>
- [12] Yin, J., Huang, L., Wu, L., Li, J., James, T.D. and Lin, W. (2021) Small Molecule Based Fluorescent Chemosensors for Imaging the Microenvironment within Specific Cellular Regions. *Chemical Society Reviews*, **50**, 12098-12150. <https://doi.org/10.1039/d1cs00645b>
- [13] Robson, J.A., Kubánková, M., Bond, T., Hendley, R.A., White, A.J.P., Kuimova, M.K., *et al.* (2020) Simultaneous Detection of Carbon Monoxide and Viscosity Changes in Cells. *Angewandte Chemie*, **132**, 21615-21619. <https://doi.org/10.1002/ange.202008224>
- [14] Wolstenholme, C.H., Hu, H., Ye, S., Funk, B.E., Jain, D., Hsiung, C., *et al.* (2020) AggFluor: Fluorogenic Toolbox Enables Direct Visualization of the Multi-Step Protein Aggregation Process in Live Cells. *Journal of the American Chemical Society*, **142**, 17515-17523. <https://doi.org/10.1021/jacs.0c07245>
- [15] Cheng, D., Xu, W., Gong, X., Yuan, L. and Zhang, X. (2021) Design Strategy of Fluorescent Probes for Live Drug-Induced Acute Liver Injury Imaging. *Accounts of Chemical Research*, **54**, 403-415. <https://doi.org/10.1021/acs.accounts.0c00646>
- [16] Chao, J., Liao, Q., Hu, L., Wang, Z., Peng, Z., Mao, G., *et al.* (2024) Near-infrared Fluorescent Probe for the Imaging of Viscosity in Fatty Liver Mice and Valuation of Drug Efficacy. *Talanta*, **276**, Article 126227. <https://doi.org/10.1016/j.talanta.2024.126227>
- [17] Fu, M., He, F., Jiang, Z., Chen, X., Xie, Z. and Hu, J. (2023) Development of a Novel Near-Infrared Molecule Rotator for Early Diagnosis and Visualization of Viscosity Changes in Acute Liver Injury Models. *RSC Advances*, **13**, 26247-26251. <https://doi.org/10.1039/d3ra04391f>
- [18] 雷玮, 王丹丹, 葛广波, 等. 肝损伤血清标志物研究进展[J]. 实用肝脏病杂志, 2017, 20(2): 252-256.
- [19] Dai, B., Jiang, S., Wang, W., Li, Z. and Feng, G. (2025) Decreased Lysosomal Polarity during Acute Alcoholic Liver Injury Revealed by a Near-Infrared Fluorescent Probe. *Analytical Chemistry*, **97**, 17102-17110. <https://doi.org/10.1021/acs.analchem.5c02887>
- [20] Zhang, Y., Jiang, Q., Wang, K., Fang, Y., Zhang, P., Wei, L., *et al.* (2024) Dissecting Lysosomal Viscosity Fluctuations in Live Cells and Liver Tissues with an Ingenious NIR Fluorescent Probe. *Talanta*, **272**, Article 125825. <https://doi.org/10.1016/j.talanta.2024.125825>
- [21] Yang, H., Chen, Y., He, J., Li, Y. and Feng, Y. (2025) Advances in the Diagnosis of Early Biomarkers for Acute Kidney Injury: A Literature Review. *BMC Nephrology*, **26**, Article No. 115. <https://doi.org/10.1186/s12882-025-04040-3>
- [22] Li, N., Liu, Z., Chen, C., Jiang, H., Liu, Y. and Ni, D. (2025) Activatable Fluorescent Ratiometric Probes for Early Diagnosis and Prognostic Assessment of Acute Kidney Injury. *Science Advances*, **11**, eaea1654. <https://doi.org/10.1126/sciadv.aea1654>
- [23] Wu, Q., Zhou, Q., Li, W., Ren, T., Zhang, X. and Yuan, L. (2022) Evolving an Ultra-Sensitive Near-Infrared  $\beta$ -Galactosidase Fluorescent Probe for Breast Cancer Imaging and Surgical Resection Navigation. *ACS Sensors*, **7**, 3829-3837. <https://doi.org/10.1021/acssensors.2c01752>
- [24] Lei, P., Wang, R., Dong, C., Shuang, S. and Li, M. (2024) Mitochondria-Targeted NIR Molecular Probe for Detecting Viscosity of Gland Damage and SO<sub>2</sub> in Actual Samples. *Journal of Industrial and Engineering Chemistry*, **140**, 658-664. <https://doi.org/10.1016/j.jiec.2024.09.046>
- [25] Xu, S., Liu, H., Yin, X., Yuan, L., Huan, S. and Zhang, X. (2019) A Cell Membrane-Anchored Fluorescent Probe for Monitoring Carbon Monoxide Release from Living Cells. *Chemical Science*, **10**, 320-325. <https://doi.org/10.1039/c8sc03584a>

- [26] Zhang, J., Zhu, X., Hu, X., Liu, H., Li, J., Feng, L., *et al.* (2016) Ratiometric Two-Photon Fluorescent Probe for *in Vivo* Hydrogen Polysulfides Detection and Imaging during Lipopolysaccharide-Induced Acute Organs Injury. *Analytical Chemistry*, **88**, 11892-11899. <https://doi.org/10.1021/acs.analchem.6b03702>
- [27] Huang, J. and Pu, K. (2021) Near-Infrared Fluorescent Molecular Probes for Imaging and Diagnosis of Nephro-Urological Diseases. *Chemical Science*, **12**, 3379-3392. <https://doi.org/10.1039/d0sc02925d>
- [28] Yang, M., Huang, J., Fan, J., Du, J., Pu, K. and Peng, X. (2020) Chemiluminescence for Bioimaging and Therapeutics: Recent Advances and Challenges. *Chemical Society Reviews*, **49**, 6800-6815. <https://doi.org/10.1039/d0cs00348d>
- [29] Feng, Y., Nie, G., Liang, W., Li, W., Zhang, Y., Wang, K., *et al.* (2022) Real-Time Imaging of Acute Alcoholic Liver Injury *in Vivo* via a Robust Viscosity Probe with Aggregation-Induced Emission Nature. *Sensors and Actuators B: Chemical*, **355**, Article 131285. <https://doi.org/10.1016/j.snb.2021.131285>
- [30] Yin, J., Xu, L., Yang, H., Qi, W., Ren, X., Zheng, X., *et al.* (2023) Construction of a Label-Detection Integrated Visual Probe to Reveal the Double-Edged Sword Principle of Ferroptosis in Liver Injury. *Analytical Chemistry*, **96**, 355-363. <https://doi.org/10.1021/acs.analchem.3c04335>
- [31] Dou, K., Huang, W., Xiang, Y., Li, S. and Liu, Z. (2020) Design of Activatable NIR-II Molecular Probe for *in Vivo* Elucidation of Disease-Related Viscosity Variations. *Analytical Chemistry*, **92**, 4177-4181. <https://doi.org/10.1021/acs.analchem.0c00634>
- [32] Peng, C., Ma, X., Lin, D., Feng, X., Yu, H. and Li, Y. (2021) A Novel Near-Infrared Viscosity Probe Based on Synergistic Effect of AIE Property and Molecular Rotors for Mitophagy Imaging during Liver Injury. *Analytica Chimica Acta*, **1187**, Article 339146. <https://doi.org/10.1016/j.aca.2021.339146>
- [33] Zhou, Y., Liu, Z., Qiao, G., Tang, B. and Li, P. (2021) Visualization of Endoplasmic Reticulum Viscosity in the Liver of Mice with Nonalcoholic Fatty Liver Disease by a Near-Infrared Fluorescence Probe. *Chinese Chemical Letters*, **32**, 3641-3645. <https://doi.org/10.1016/j.cclet.2021.04.035>
- [34] Tang, Y., Peng, J., Zhang, Q., Song, S. and Lin, W. (2022) A New NIR Emission Mitochondrial Targetable Fluorescent Probe and Its Application in Detecting Viscosity Changes in Mouse Liver and Kidney Injury. *Talanta*, **249**, Article 123647. <https://doi.org/10.1016/j.talanta.2022.123647>
- [35] Peng, H., Jing, X., Han, S. and Lin, W. (2024) Detecting Viscosity Changes in the Limb Ischemia-Reperfusion in Mice with a Near-Infrared Fluorescence Probe. *Analytica Chimica Acta*, **1311**, Article 342733. <https://doi.org/10.1016/j.aca.2024.342733>
- [36] Wang, X., Yin, Z., Liu, H., Wang, Z., Zhu, X. and Ye, Y. (2024) A Novel NIR Fluorescence Probe with AIE Property to Image Viscosity in Nystatin-Induced Cell Model. *Journal of Fluorescence*, **35**, 2935-2942. <https://doi.org/10.1007/s10895-024-03706-9>
- [37] Liao, Q., Chao, J., Wang, W., Liu, T., Mao, G., Xu, F., *et al.* (2023) A Novel Near-Infrared Fluorescent Probe for the Imaging of Viscosity in Cells and Tumor-Bearing Mice. *Chemical Communications*, **59**, 5607-5610. <https://doi.org/10.1039/d3cc01101a>
- [38] Zhang, X., He, X., Si, Y., Nie, X., Lun, S., Wang, C., *et al.* (2025) A Dual Sensitive Fluorescence Probe for the Simultaneous Visualization of Hypochlorite and Viscosity in Living Cells and Zebrafish. *Spectrochimica Acta Part A: Molecular and Biomolecular Spectroscopy*, **325**, Article 125149. <https://doi.org/10.1016/j.saa.2024.125149>